J|A|C|S
ARTICLES
Published on Web 02/01/2008

Stable Luminescence from Individual Carbon Nanotubes in Acidic, Basic, and Biological Environments

Juan G. Duque,[†,‡] Laurent Cognet,*[,§,||] A. Nicholas G. Parra-Vasquez,[†,‡] Nolan Nicholas,[‡,⊥] Howard K. Schmidt,*[,‡] and Matteo Pasquali*[,†,‡,§]

Department of Chemical and Biomolecular Engineering, Carbon Nanotechnology Laboratory, The Smalley Institute for Nanoscale Science and Technology, Department of Chemistry, and Department of Physics and Astronomy, Rice University, 6100 Main Street, Houston, Texas 77005, and Centre de Physique Moléculaire Optique et Hertzienne, Université Bordeaux 1 and CNRS, Talence F-33405, France

Received October 15, 2007; E-mail: lcognet@u-bordeaux1.fr; hks@rice.edu; mp@rice.edus

Abstract: Aqueous surfactant suspensions of single walled carbon nanotubes (SWNTs) are very sensitive to environmental conditions. For example, the photoluminescence of semiconducting SWNTs varies significantly with concentration, pH, or salinity. In most cases, these factors restrict the range of applicability of SWNT suspensions. Here, we report a simple strategy to obtain stable and highly luminescent individualized SWNTs at pH values ranging from 1 to 11, as well as in highly saline buffers. This strategy relies on combining SWNTs previously suspended in sodium dodecylbenzene sulfonate (SDBS) with biocompatible poly(vinyl pyrrolidone) (PVP), which can be polymerized in situ to entrap the SWNT-SDBS micelles. We present a model that accounts for the photoluminescence stability of these suspensions based on PVP morphological changes at different pH values. Moreover, we demonstrate the effectiveness of these highly stable suspensions by imaging individual luminescent SWNTs on the surface of live human embryonic kidney cells (HEK cells).

Introduction

Single walled carbon nanotubes (SWNTs) are one of the most interesting classes of nano-objects due to their unique thermal, physical, optical, and electronic properties.[1−6] SWNTs can exhibit metallic-, semimetallic-, or semiconductor-type behavior depending on their chirality, conceptualized by the twist angle of a graphene sheet rolled to form a tube. A striking example of SWNT chirality-dependent properties is the near-infrared (near-IR) luminescence of semiconducting species. The spectroscopic signatures of SWNTs depend on their environment.[7−9] For example, changes in the surroundings, such as acidification, can induce bleaching of their UV−vis absorption, quenching of their fluorescence, and shifting of their spectra. These manifestations can be used to monitor electron transfer, protonation, and charge-transfer reactions[9−12] and even individual molecular reactions.[13] However, the pronounced sensitivity of SWNT optical and electronic properties to their environment is not always desirable because it might restrict or prevent altogether their use in some of the most promising applications, especially in biological systems including drug delivery, biosensors, biomedical devices, and cell biology.[1,4,14] Viable cells and tissues require specific environmental conditions such as temperature, salt concentration, and pH; these variables influence to various degrees the spectral properties of SWNT suspensions.[10,15,16] None of the SWNT wrapping strategies proposed to date provides highly luminescent tubes across these conditions.

Surfactants are routinely used to suspend and isolate SWNTs in aqueous environments, enabling examination of their pho-

[†] Department of Chemical and Biomolecular Engineering, Rice University.
[‡] The Smalley Institute for Nanoscale Science and Technology, Rice University.
[§] Department of Chemistry, Rice University.
[||] Université Bordeaux 1 and CNRS.
[⊥] Department of Physics and Astronomy, Rice University.

(1) Sinnott, S. B.; Andrews, R. *Crit. Rev. Solid State Mater. Sci.* **2001**, *26*, 145−249.
(2) Khan, Z. H.; Husain, B. *Indian J. Eng. Mater. Sci.* **2005**, *12*, 529−551.
(3) Setton, R. *Carbon* **1995**, *33*, 135−140.
(4) Dai, H. J. *Surf. Sci.* **2002**, *500*, 218−241.
(5) Baughman, R. H.; Zakhidov, A. A.; de Heer, W. A. *Science* **2002**, *297*, 787−792.
(6) Banks, M. G. *Scientometrics* **2006**, *69*, 161−168.
(7) Ohno, Y.; Iwasaki, S.; Murakami, Y.; Kishimoto, S.; Maruyama, S.; Mizutani, T. *Phys. Rev. B* **2006**, *73*, 235427.
(8) O'Connell, M.; Bachilo, S. M.; Huffman, C.; Moore, V. C.; Strano, M. S.; Haroz, E.; Rialon, K. L.; Boul, P.; Noon, W. H.; Kittrell, C.; Ma, J.; Hauge, R. H.; Weisman, R. B.; Smalley, R. *Science* **2002**, *297*, 593−596.
(9) Zhang, M.; Yudasaka, M.; Miyauchi, Y.; Maruyama, S.; Iijima, S. *J. Phys. Chem. B* **2006**, *110*, 8935−8940.
(10) Strano, M. S.; Huffman, C. B.; Moore, V. C.; O'Connell, M. J.; Haroz, E. H.; Hubbard, J.; Miller, M. K.; Rialon, K. L.; Kittrell, C.; Ramesh, S.; Hauge, R. H.; Smalley, R. E. *J. Phys. Chem. B* **2003**, *107*, 6979−6985.
(11) O'Connell, M. J.; Eibergen, E. E.; Doorn, S. K. *Nat. Mater.* **2005**, *4*, 412−418.
(12) Lee, C. Y.; Baik, S.; Zhang, J. Q.; Masel, R. I.; Strano, M. S. *J. Phys. Chem. B* **2006**, *110*, 11055−11061.
(13) Cognet, L.; Tsyboulski, D. A.; Rocha, J.-D. R.; Doyle, C. D.; Tour, J. M.; Weisman, R. B. *Science* **2007**, *316*, 1465−1468.
(14) Palwai, N. R.; Martyn, D. E.; Neves, L. F. F.; Tan, Y.; Resasco, D. E.; Harrison, R. G. *Nanotechnology* **2007**, *18*, 235601.
(15) Nish, A.; Nicholas, R. J. *Phys. Chem. Chem. Phys.* **2006**, *8*, 3547−3551.
(16) Niyogi, S.; Boukhalfa, S.; Chikkannanavar, S. B.; McDonald, T. J.; Heben, M. J.; Doorn, S. K. *J. Am. Chem. Soc.* **2007**, *129*, 1898−1899.

toluminescence properties.[8,17] Anionic surfactants are the most widely employed, and SDBS is generally preferred because it gives the most blue-shifted resonances and high luminescent yields from the suspended SWNTs. Although surfactant wrapped SWNTs are stable in aqueous suspensions, slight changes in the pH of the solution affects the photoluminescence of the SWNTs (especially decreases toward acidity) and can even destabilize the suspension and cause flocculation.[10,13,18] The bleaching of the fluorescence of sodium dodecyl sulfate (SDS) or sodium dodecylbenzene sulfonate (SDBS) suspended nanotubes in acidic media was attributed to the selective protonation of pre-adsorbed oxygen at the SWNT sidewalls; the protonation could be reversed by readjusting the solution pH from acidic to alkaline. Interestingly, a partial restoration of the absorption and fluorescence spectrum was observed after the addition of poly(vinyl pyrrolidone) (PVP); this was attributed to a strong interaction between the interface of the SDS micelles and PVP molecules that had been documented previously.[10,19−22] The luminescence properties of nanotube suspensions are also strongly dependent on surfactant concentration.[23] Below the critical micelle concentration (cmc), substantial red-shifts, fluorescence reduction, and eventual flocculation are observed in the suspension.[10] An additional drawback concerning the use of surfactants alone is that they are not biocompatible. To overcome this limitation, biocompatible SWNT suspensions were recently obtained and thought to result from the nonspecific replacement of a Pluronics polymer wrapping by unidentified proteins in biological sera. This strategy is, however, not universal and produces weakly luminescent SWNTs.[24]

Here, we report a new strategy to obtain suspensions of highly luminescent SWNTs using a combination of surfactant (SDBS) and a biocompatible polymer (PVP) or by polymerizing in situ its monomer vinyl pyrrolidone (ISPVP). This results in nanotube suspensions with the optimal luminescent properties of SDBS-SWNT suspensions at any pH value between 1 and 11. We combine literature evidence of the strong PVP-SDBS micelle surface interaction together with SWNT spectroscopic signatures and different types of single molecule images to propose a model explaining the behavior of PVP-SDBS-SWNT at neutral and low pH values. The suspensions remain stable (for weeks) at all pH values as well as in saline buffers. Importantly, they are also stable after extended dialysis (below the cmc of SDBS) and retain fluorescence after lyophilization and resuspension in deionized water (DI). This should open many applications in biology because the nanotubes can be suspended in a biocompatible environment. Using individual SWNT near-IR photoluminescence microscopy, we show that ISPVP-SDBS-SWNT suspensions are stable and strongly luminescent in living cell cultures, where they interact efficiently on cell membranes and do not display any sign of aggregation.

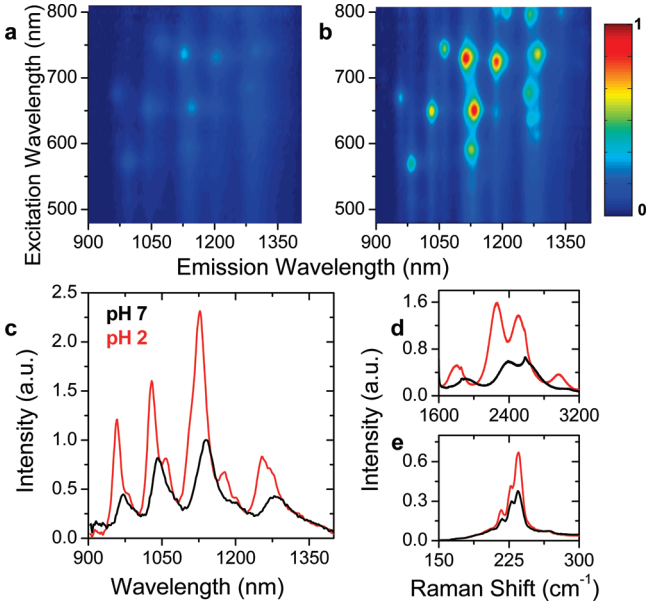

Figure 1. Ensemble spectroscopic measurements of PVP-SDBS-SWNT in neutral and acidic conditions. (a and b) Contour plots of fluorescence intensity vs excitation and emission wavelength of PVP-SDBS-SWNT at pH 7 (a) and 2 (b). Identical intensity scales are used in panels a and b. (c) Fluorescence spectra obtained from excitation at 660 nm from PVP-SDBS-SWNT at pH 7 (black) and 2 (red). (d and e) Liquid-phase Raman spectroscopy using excitation at 785 nm (see text). Fluorescence (d) and RBM (e) spectra obtained at pH 7 (black) and 2 (red).

Results and Discussion

The PVP-SDBS-SWNT suspensions studied here were prepared in two steps. First, raw HiPco SWNTs were dispersed in SDBS (1 wt %) through a standard decanting procedure (see Experimental Procedures). Second, a fraction of the suspension was mixed with a 1 wt % solution of PVP (55 kDa, unless otherwise stated) to obtain a surfactant-polymer complex. The variations of the luminescent properties of PVP-SDBS-SWNT suspensions with pH are presented in Figure 1. Figure 1a,b shows the 2-D contour plots of the fluorescence intensity versus the excitation and emission wavelength before (Figure 1a) and after (Figure 1b) the addition of HCl (1 N) to reach a final pH of 2. Strikingly, the addition of acid enhanced the luminescence intensity at every wavelength. For a simpler quantitative analysis, the emission spectra of the semiconducting SWNT obtained from excitation at 660 nm are displayed (Figure 1c). The spectra were normalized to the maximum intensity peak at 1120 nm of the initial suspension, which can be assigned to the (7,6) tube.[25] Upon acidification, the fluorescence intensity was enhanced approximately by a factor of 2. Interestingly, this enhancement was accompanied by a narrowing and blue-shift (~25 nm) of every peak. To complement these observations, the liquid-phase Raman spectra of the suspensions were also measured. Using 785 nm excitation, which selectively excites semiconducting nanotubes with diameters near 1 nm,[10] we studied the radial breathing modes (RBM, 100−300 cm^{-1})[26] as well as fluorescence in the 1620−3200 cm^{-1} range. The fluorescence obtained by liquid-phase Raman (Figure 1d) confirmed the previous observations (Figure 1c). The degree of bundling could be monitored by comparing the area under

(17) Bachilo, S. M.; Strano, M. S.; Kittrell, C.; Hauge, R. H.; Smalley, R. E.; Weisman, R. B. *Science* **2002**, *298*, 2361−2366.
(18) Wang, D.; Chen, L. *Nano Lett.* **2007**, *7*, 1480−1484.
(19) Atkin, R.; Bradley, M.; Vincent, B. *Soft Matter* **2005**, *1*, 160−165.
(20) Zhai, L. M.; Lu, X. H.; Chen, W. J.; Hu, C. B.; Zheng, L. *Colloids Surf., A* **2004**, *236*, 1−5.
(21) Brackman, J. C.; Engberts, J. *Chem. Soc. Rev.* **1993**, *22*, 85−92.
(22) Zanette, D.; Froehner, S. J.; Minatti, E.; Ruzza, A. A. *Langmuir* **1997**, *13*, 659−665.
(23) McDonald, T. J.; Engtrakul, C.; Jones, M.; Rumbles, G.; Heben, M. J. *J. Phys. Chem. B* **2006**, *110*, 25339−25346.
(24) Cherukuri, P.; Gannon, C. J.; Leeuw, T. K.; Schmidt, H. K.; Smalley, R. E.; Curley, S. A.; Weisman, B. *Proc. Natl. Acad. Sci. U.S.A.* **2006**, *103*, 18882−18886.
(25) Weisman, R. B.; Bachilo, S. M.; Tsyboulski, D. *Appl. Phys. A: Mater. Sci. Process.* **2004**, *78*, 1111−1116.
(26) Heller, D. A.; Barone, P. W.; Swanson, J. P.; Mayrhofer, R. M.; Strano, M. S. *J. Phys. Chem. B* **2004**, *108*, 6905−6909.

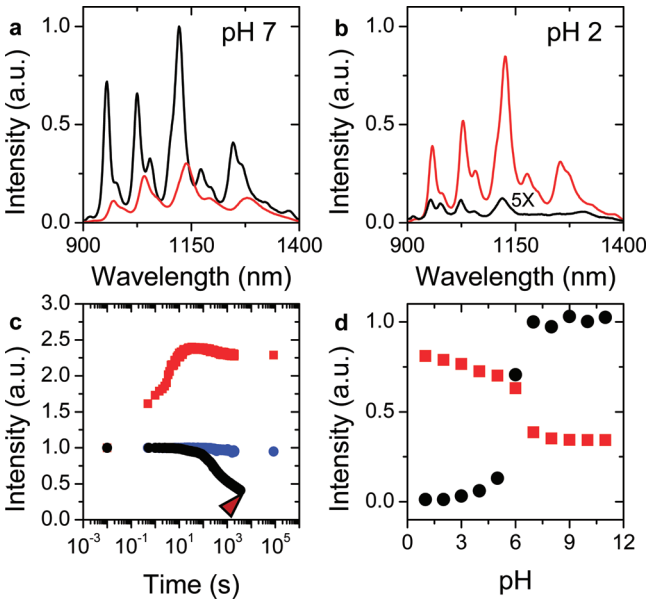

Figure 2. Comparison of SDBS-SWNT, PVP-SWNT, and PVP-SDBS-SWNT fluorescence ensemble properties. (a and b) Comparative fluorescence spectra recorded at pH 7 (a) and 2 (b) from SDBS-SWNT (black curves) and PVP-SDBS-SWNT (red curves). All spectra were normalized to absorbance at 763 nm. (c) Kinetic time course of the (7,6) fluorescence peak intensity (1120 nm) for the three different SWNT suspensions following the addition of acid. SDBS-SWNT in black, PVP-SWNT in blue, and PVP-SDBS-SWNT in red. The triangle indicates occurrence of flocculation of the SDBS-SWNT suspension. (d) Steady state fluorescence intensity of the (7,6) peak of SDBS-SWNT (black) and PVP-SDBS-SWNT (red) as a function of pH. All steady state values were normalized to SDBS-SWNT at pH 7.

the RBM of individual semiconducting SWNTs (150−250 cm^{-1}) with that of SWNTs that are brought into resonance with the laser due to the presence of SWNT bundles (250−300 cm^{-1}).[26−29] The RBM area of the individual SWNTs increased after acidification (Figure 1e), suggesting that a subtle change in the SWNT immediate environment had occurred. The degree of bundling, however, was unchanged because the bundling peak remained constant. Moreover, the location and amplitude of the G-peak (not shown) remained constant after acidification, indicating that the SWNTs were not protonated.[10] A variety of acids besides HCl (phosphoric, nitric, and sulfuric acid) was surveyed, and similar fluorescence enhancements and spectral shifts were observed with each. Analogous effects were obtained using SDS instead of SDBS. Altogether, these observations support the notion that at low pH values, PVP-SDBS-SWNTs remain individual and that a change must occur in the close environment of the SWNTs.

To elucidate further the mechanism of PVP-SDBS-SWNT luminescence enhancement upon acidification, we compared the behavior of SDBS-SWNT, PVP-SWNT, and PVP-SDBS-SWNT suspensions. Figure 2a,b displays the fluorescence spectra of SDBS-SWNT (black curve) and PVP-SDBS-SWNT (red curve) recorded at pH 7 (a) and 2 (b) after normalization to the (7,6) SWNT for SDBS at pH 7. The spectra in Figure 2a indicate that when PVP is added to SDBS-SWNTs, the fluorescence peaks decrease in intensity, red-shift, and broaden.[8] Thus, the addition of PVP at pH 7 strongly affects the luminescence properties of SDBS-SWNTs. When acidified to pH 2, SDBS-SWNT solutions bleach partially, in analogy with previously reported data for SDS,[10] to an extent that is dependent on the tube diameter (Figure 2b). As discussed previously, the PVP-SDBS-SWNT suspension displayed the opposite trend when acidified down to pH 2 because the fluorescence was enhanced to about 80% of the level of SDBS-SWNTs at neutral conditions (pH 7). It is important to note that if PVP is added to a SDBS-SWNT suspension that was previously acidified, only a partial luminescence recovery was observed (∼10%) in accordance with previous reports.[10] Therefore, PVP must be present in the SDBS-SWNT solution before the addition of acid to obtain a suspension that is highly fluorescent at low pH values.

Figure 2c shows the kinetic time course of the (7,6) fluorescence peak intensity for the three different SWNT suspensions following the addition of acid. The fluorescence intensities were normalized to the initial condition at pH 7. For the first 200 s, the luminescence intensity of the SDBS-SWNT suspension did not evolve noticeably (black dots in Figure 2c). It then decreases substantially (with faster rates for the small band gap tubes, i.e., large diameters, not shown) before we eventually observed that the nanotubes flock out of the solution. We tentatively attribute this behavior to a slight destabilization of the SDBS micelle in acidic conditions, which creates openings through which acid can contact SWNTs and consequently quench fluorescence;[10,30] the result at low pH values is the complete destabilization of the micelles and flocculation of the SWNTs. The flocculation onset time (depicted by the triangle in Figure 2c) can vary from minutes to hours depending on the amount of acid and concentration of surfactant (not shown). Notably, the fluorescence of a neat PVP-SWNT suspension (no SDBS) is considerably weaker than that of SDBS suspended tubes (only ∼3% of that of SDBS-SWNTs at equal concentrations).[31] Nevertheless, the same acidification procedure can be performed and indicates that PVP-SWNT luminescence is barely affected by acidification: the luminescence drops only by 5% over 24 h (blue dots in Figure 2c). In clear contrast to the two preceding suspensions, PVP-SDBS-SWNTs exhibit a very different kinetic behavior upon acidification. The fluorescence peak intensity increased rapidly until it stabilized at about twice the initial fluorescence level (red dots in Figure 2c). This rapid increase suggests an entirely different mechanism than for SDBS-SWNT suspensions.

The steady fluorescence intensity levels of the (7,6) peak are presented for SDBS-SWNT (in black) and PVP-SDBS-SWNT (in red) as a function of pH (Figure 2d). Both curves were normalized to SDBS-SWNTs at neutral pH values. In both nanotube suspensions, the fluorescence remained constant between pH 11 and 7. In acidic conditions, the relative intensity of SDBS-SWNT suspensions decreased gradually as the pH was lowered to pH 1 with subsequent flocculation, whereas that of PVP-SDBS-SWNT increased continuously to reach 80% of the

(27) Doorn, S. K.; Heller, D. A.; Barone, P. W.; Usrey, M. L.; Strano, M. S. *Applied Physics A: Mater. Sci. Process.* **2004**, *78*, 1147−1155.
(28) Dyke, C. A.; Stewart, M. P.; Tour, J. M. *J. Am. Chem. Soc.* **2005**, *127*, 4497−4509.
(29) The RBM of the bundles or "bundling peak" is the excitation of metallic (11,0) and semiconducting (10,2) tubes with the 785 nm laser that are red-shifted into resonance due to the presence of bundles in the bulk solution.
(30) Dukovic, G.; White, B. E.; Zhou, Z. Y.; Wang, F.; Jockusch, S.; Steigerwald, M. L.; Heinz, T. F.; Friesner, R. A.; Turro, N. J.; Brus, L. E. *J. Am. Chem. Soc.* **2004**, *126*, 15269−15276.
(31) Obtaining a stable and highly luminescence suspension of SWNTs in PVP alone is very difficult to accomplish without the aid of previously suspended tubes in surfactants such as SDS or SDBS. The fluorescence yield of PVP wrapped tubes is only 3% of that of SDBS.

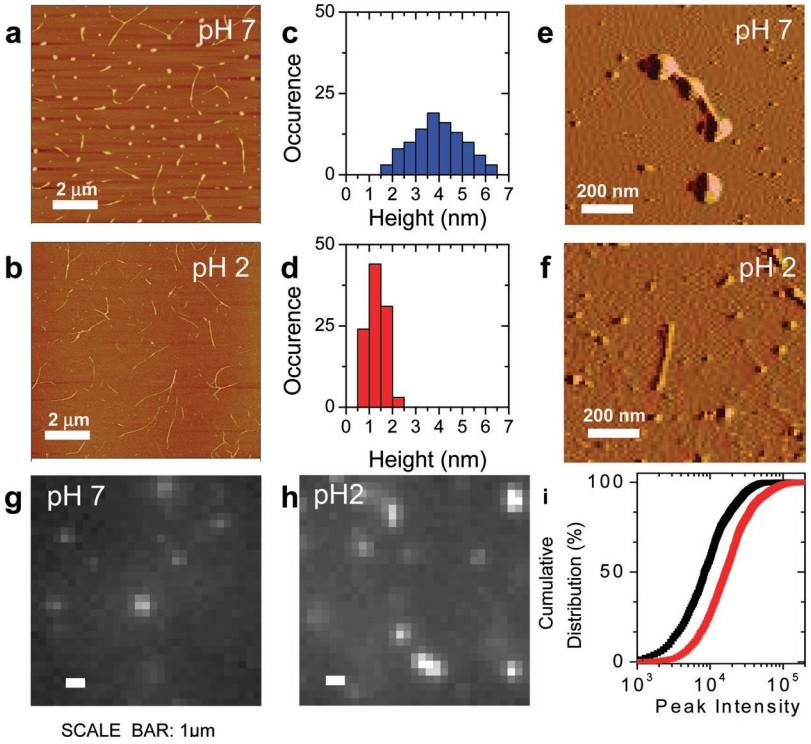

Figure 3. AFM and near-IR study of individual PVP-SDBS-SWNT. (a and b) Representative AFM images of PVP-SDBS-SWNT at pH 7 (a) and 2 (b) after surface cleaning. (c and d) Distributions of the SWNT heights measured on several similar clean AFM images at pH 7 (c) and 2 (d). (e and f) Same as in panels a and b but without surface cleaning. (g and h) Near-IR luminescence images of individual PVP-SDBS-SWNT at pH 7 (g) and 2 (h). Scale bars are 1 μm. (i) Cumulative distribution of the luminescence signal amplitudes of the peaks detected in 400 similar images as panels g and h, at pH 7 (black) and 2 (red).

luminescence level of the benchmark SDBS-SWNT suspension at pH 7. The luminescence of PVP-SDBS-SWNT remained stable for weeks over the entire pH range studied.

Finally, we tested the influence of the charge of the surfactant. When PVP is added to SWNTs initially suspended in cationic or neutral surfactants (CTAB and Pluronics), no spectral changes are observed, in stark contrast to anionic surfactants. This can be related to previous reports that showed no interactions between PVP and cationic micelles, while strong interactions between PVP and anionic micelles were observed.[20] In addition, when various types of acids were added to SWNTs suspended in cationic surfactants, efficient fluorescence bleaching was observed, comparable with previous observations[10] regardless of the presence of PVP. Altogether, our data suggest that in PVP-SDBS-SWNT suspensions, SDBS remains around the SWNTs after the addition of PVP and is not replaced by PVP. Instead, a surfactant-polymer complex is formed that wraps the SWNTs and apparently provides an efficient and stable barrier between the SWNTs and their local environment. This amounts to a bilayer assembly of complementary polymers, reminiscent of the chemistry underlying fuzzy nanoassemblies[32] and nanotube/polyelectrolyte composites[33] and suggests a perhaps general approach for engineering a variety of specialized SWNT bioplatforms.

We believe that the conformation of PVP together with its strong affinity for SDBS is at the origin of the red-shift and partial quenching of luminescence that follows the addition of PVP to SDBS-SWNTs at neutral and basic pH values (Figure 2a). PVP contains both hydrophobic and hydrophilic moieties; thus, it adopts a coiled conformation in neutral and basic solutions.[34] The strong interaction of PVP with the outer surface (due to the charge transfer between the sulfate molecule from SDBS and the nitrogen group from PVP[20]) of the SDBS micelles surrounding the SWNTs is therefore likely to destabilize slightly the micelle structures and subsequently disturb the SWNT luminescent properties. Upon acidification, PVP is known to protonate and swell.[19] This conformational change (Figure 2c) allows SDBS to reform its ideal micelle structure around the SWNT, rewrapping it completely. This seems to occur before the incoming acid could destabilize the micelle and quench the SWNT luminescence because this would occur at a longer time scale (Figure 2c). In this model, the stabilizing layer (PVP) prevents any disruption of the micelles, and the luminescence that is obtained in acidic environments is comparable to that of SDBS-SWNTs at basic conditions.

The model presented previously was deduced from spectroscopic measurements of bulk suspensions. To test it, we used several imaging techniques that can probe the environmental and photophysical properties of individual nanotubes. Figure 3a,b shows AFM images of nanotubes prepared under basic and acidic conditions. To allow a statistical analysis of a large number of tubes, AFM images were primarily acquired on samples that were cleaned to remove the excess of PVP and SDBS (see Experimental Procedures). It should be noted that it was more difficult to obtain clean surfaces at neutral conditions at which the excess of surfactant could not be fully removed, as compared to acidic conditions (Figure 3a,b). Close examina-

(32) Decher, G. *Science* **1997**, *277*, 1232−1237.
(33) Mamedov, A. A.; Kotov, N. A.; Prato, M.; Guldi, D. M.; Wicksted, J. P.; Hirsch, A. *Nat. Mater.* **2002**, *1*, 190−194.
(34) Khanal, A.; Li, Y.; Takisawa, N.; Kawasaki, N.; Oishi, Y.; Nakashima, K. *Langmuir* **2004**, *20*, 4809−4812.

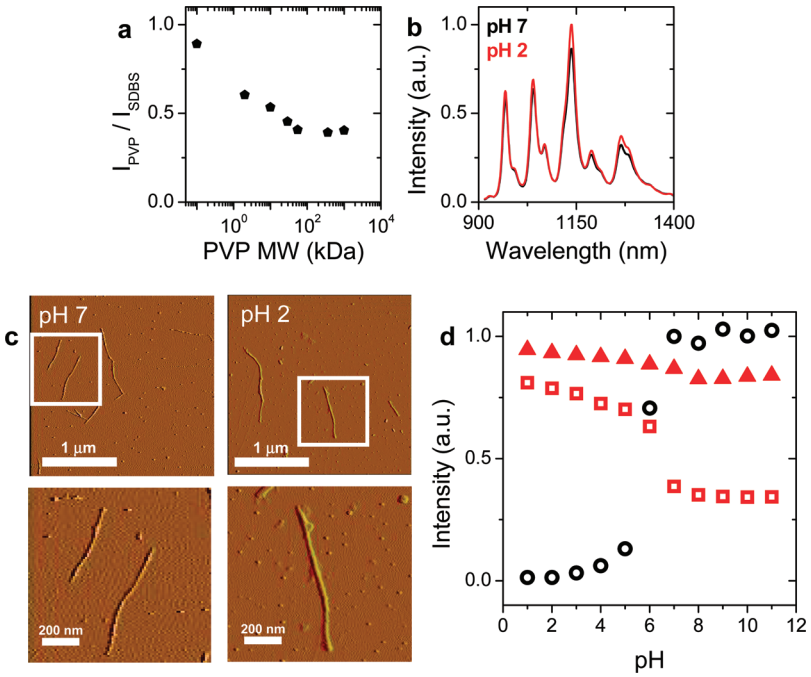

Figure 4. Fluorescence properties and AFM images of VP-SDBS-SWNT. (a) Ratio of the integrated areas of the fluorescence of PVP at different molecular weights to SDBS at 660 nm excitation and pH 7. (b) Fluorescence of VP-SDBS-SWNT at neutral (in black) and acidic (in red) conditions. (c) AFM images of covered SWNT with VP after surface cleaning. (d) Effect of pH to the relative intensity of the (7,6) peak of VP-SDBS-SWNT suspensions (red triangles, open symbols are previously shown data in Figure 2d).

tion of these images indicates that the vast majority of the tubes is individual. This conclusion was also confirmed by Cryo-TEM (see Supporting Information Figure S1). The quantifications of the apparent nanotube height at pH 7 (3.9 ± 0.1 nm, $\pm$ standard error of the mean (SEM), $n = 102$) and at pH 2 (1.3 ± 0.04 nm, $n = 102$) indicate that nanotubes are surrounded by a bulkier structure at pH 7 than at pH 2 (Figure 3c,d). To rule out the effect of the cleaning procedure, and to obtain a more precise picture of the PVP-SDBS structure around the nanotubes, we obtained AFM images using samples that had not been pre-cleaned. Examples of tubes isolated from the excess of the surfactant-polymer mixture are presented in Figure 3e,f. The different conformations of PVP-SDBS presented in our model are now evident: at pH 7, large agglomerates (>10 nm) are present on the SWNTs, whereas at pH 2, a more uniform and thinner coverage is observed (6 nm).

The photoluminescence of the SWNT suspensions was investigated further by direct visualization in a near-IR microscope.[35] Figure 3g,h shows snapshots obtained from dilute PVP-SDBS-SWNT suspensions in neutral and acidic conditions. The majority of the luminescence spots is likely to originate from individual SWNTs.[8,35] and is diffraction limited (2 pixels correspond to 670 nm in Figure 3g,h), which indicates that most of the spots have a length shorter than 670 nm. In these images, the luminescence spots appear to be brighter in the acid suspension than in the neutral suspension. This observation is quantified by computing and comparing the cumulative distributions of the individual fluorescent spot signal amplitudes obtained in the two conditions (Figure 3i).[36] The signals were obtained from the statistical fit of each spot's spatial distribution by a 2-D Gaussian function.[37] The widths of the distributions were identical and broad. This dispersion in signal amplitudes is likely due to the heterogeneity in the length and electronic structure of the SWNTs present in the sample. The distribution of the acidic suspension (shown in red in Figure 3i) is, however, shifted toward higher luminescence signals as compared to the neutral condition (shown in black in Figure 3i). This indicates that the luminescence of each individual PVP-SDBS-SWNT is enhanced in acidic conditions. More precisely, the ratio of the median value of the two distributions is equal to 1.9, in good agreement with the fluorescence enhancement observed in bulk using the same excitation at 660 nm wavelength (Figure 1c).

To examine the hypothesis that coiled PVP disrupts the SDBS micelle conformation at pH 7, causing the SWNT luminescence peaks to red-shift, broaden, and decrease in intensity as compared to SDBS tubes alone, we examined the influence of the PVP molecular weight (MW). Figure 4a shows the ratio of the integrated area of PVP-SDBS-SWNT to SDBS-SWNT fluorescence (excited at 660 nm) measured at pH 7 as a function of the PVP MW (from the monomer VP to 1 MDa). This ratio decreased with the MW in the range of the monomer to polymers of about 55 kDa. This spectroscopic dependence on MW indicates that the size, and certainly the conformation, of PVP has a significant effect on the optical properties of the SWNTs. Moreover, we found that the arrangement of PVP on the SDBS-SWNT complex could be controlled by polymerizing the monomer VP directly on the micelle. VP is known to undergo cationic polymerization;[38] this process is slow at pH 7 but progresses rapidly at low pH values (see Supporting Information). Therefore, we made in situ polymerized PVP (ISPVP) by introducing VP at pH 7, allowing sufficient time for the diffusion of VP to the micelles, and subsequently

(35) Tsyboulski, D. A.; Bachilo, S. M.; Weisman, R. B. *Nano Lett.* **2005**, *5*, 975−979.
(36) Schmidt, T.; Schutz, G. J.; Baumgartner, W.; Gruber, H. J.; Schindler, H. *J. Phys. Chem.* **1995**, *99*, 17662−17668.
(37) Schmidt, T.; Schutz, G. J.; Baumgartner, W.; Gruber, H. J.; Schindler, H. *Proc. Natl. Acad. Sci. U.S.A.* **1996**, *93*, 2926−2929.
(38) Stevens, M. P. *Polymer Chemistry: An Introduction*, 3rd ed.; Oxford University Press: New York, 1999.

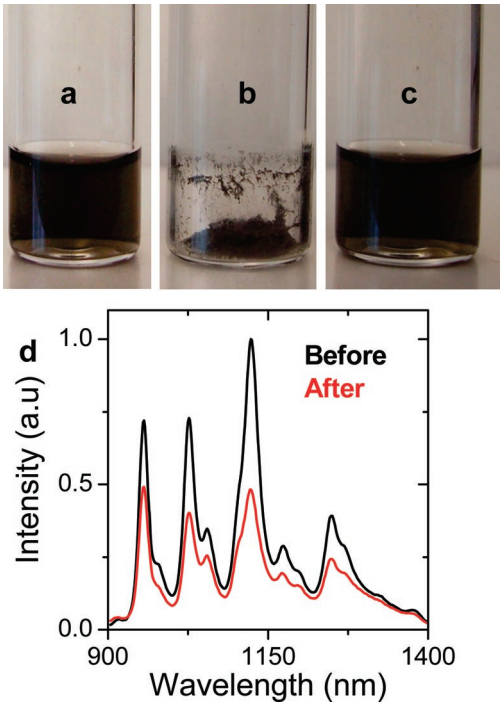

Figure 5. Lyophilized ISPVP-SDBS-SWNTsuspension. (a) ISPVP-SDBS-SWNT suspension. (b) Lyophilized ISPVP-SDBS-SWNT suspension. (c) Resuspended ISPVP-SDBS-SWNT suspension. (d) Fluorescence spectra before and after lyophilization.

acidifying the solution, causing complete polymerization of the VP and entrapping the SDBS-SWNT complex (complete polymerization of VP is also important because the VP monomer is carcinogenic, whereas PVP is harmless). Importantly, once the VP was polymerized in situ in acid conditions, the fluorescence intensity remained constant when the solution was returned to basic conditions (see Supporting Information Figure S3).

On the basis of the behavior at neutral pH values, ISPVP or very small PVP chains should yield encapsulated PVP-SDBS-SWNTs with ideal spectroscopic properties. This is indeed the case. First, the fluorescence intensity of the VP-SDBS-SWNT suspensions is almost constant (red triangles in Figure 4d) from alkaline (pH 11) to acidic (pH 1) conditions. This is in contrast to the behavior of SDBS-SWNTs (black circles) and PVP-SDBS-SWNTs (red squares) as previously discussed in Figure 2d. Second, VP-SDBS-SWNTs display essentially the optimal luminescence properties of SDBS-SWNT suspensions (narrow and almost identical peak positions) but in the whole pH range investigated (Figure 4b). The residual small red-shifts (<10 nm) together with the absence of the effect of pH suggest that ISPVP interacts strongly with the SDBS micelles but without disrupting the SDBS micelle conformation (see more details about ISPVP in the Supporting Information). AFM images support this picture since individual IPSPVP-SDBS-SWNTs are found with a uniformly thin coating (typically 5 nm) along their surface (Figure 4c). ISPVP can serve as an alternative method for producing non-covalent encapsulated SWNTs whose intrinsic properties are retained in different environments.[39,40] Control experiments with pyrrolidone molecules that do not polymerize under acidic conditions (i.e., 1-methyl-2-pyrrolidone (NMP) and *N*-ethyl-2-pyrrolidone) did not show protection at low pH values. To further examine the stability of the polymer wrapped SDBS-SWNTs system, we freeze-dried the ISPVP-SDBS-SWNT suspensions (see Experimental Procedures) at neutral pH and resuspended them in DI water. Figure 5a−c shows that the ISPVP-SDBS-SWNT suspension can be lyophilized completely and then readily resuspended in water by mild shaking. The positions of the spectroscopic peaks (absorbance, liquid-phase Raman, and fluorescence) remain unchanged; their relative fluorescence intensities after resuspension are approximately 75% of the initial intensity (Figure 5d). Such a small loss in intensity after resuspension may be due to the formation of small flocs of a few polymer wrapped SWNTs during the freeze-drying process; however, inspection by bright-field optical microscopy (63×) did not reveal any structures. The retention of nearly all of the near-IR fluorescence after resuspension confirms that ISPVP encapsulates the SDBS-SWNTs effectively

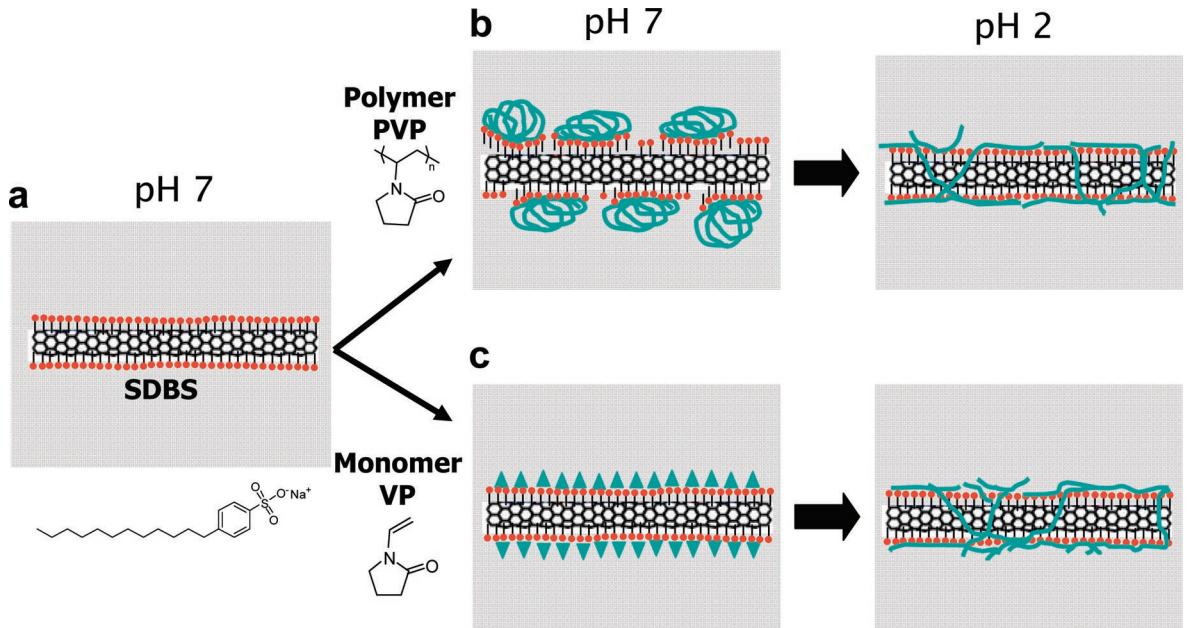

Figure 6. Schematic illustration of the model. (a) SDBS-SWNT at pH 7. (b) PVP-SDBS-SWNT at pH 7 and 2. (c) VP-SDBS-SWNT at pH 7 and 2 for which cationic polymerization occurred. See text and Supporting Information for details.

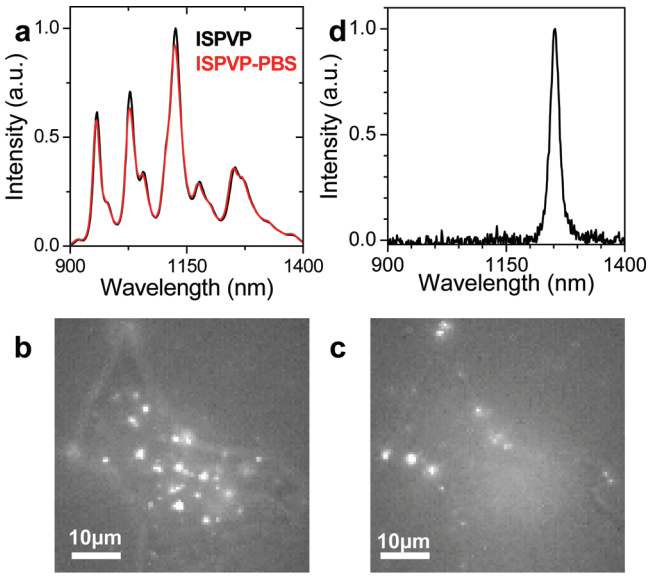

Figure 7. VP-SDBS-SWNT in biological environments. (a) Comparative fluorescence spectra of VP-SDBS-SWNT recorded in water at pH 7 (in black) and in 10× PBS (in red) at identical concentrations. (b and c) Near-IR luminescence images of the same cell incubated for 5 min with ISPVP-SDBS-SWNT at different foci: at the apical membrane (b) and at the surface of the coverslip (c). The luminescence images were acquired in the presence of white light to identify the outline of the cell. Scale bars are 10 μm. (d) Narrow spectrum measured from a luminescence spot identified at the surface of a cell, a signature of individual ISPVP-SDBS-SWNTs.

without affecting the pristine electronic structure of the SWNT. In contrast, resuspension of SDBS-SWNTs after freeze-drying is not feasible.

A schematic of the model proposed in this work is presented in Figure 6. This model shows that PVP or VP adsorbs strongly to the external surface of the SDBS micelle due to charge transfer between the sulfate group of SDBS and the nitrogen of PVP and/or VP. At neutral pH values, the conformational state of PVP slightly disrupts the micelle conformation of SDBS and subsequently disturbs the SWNT luminescent properties, while the monomer does not, as previously discussed. In acidic conditions, conformational changes of PVP and VP polymerization make both VP and PVP efficient wrappers of the SDBS-SWNTs, without displacing the SDBS micelle. The resulting surfactant-polymer complex that surrounds the SWNTs efficiently provides a stable barrier between the SWNTs and their local environment. Interestingly, this model implies that the ISPVP-SDBS interactions strengthen the micellar structure and therefore should protect the tube luminescence properties from different types of environmental factors, which would benefit important applications. Along this line, we first tested the luminescence stability of the ISPVP-SDBS-SWNT suspension far below the cmc of SDBS (~0.25 wt %). The suspensions remained stable and luminescent upon dilutions down to 1.25×10^{-4} wt % SDBS, after which any further dilution prevented accurate fluorescence measurements (not shown). We then tested the effect of salinity on the stability of the suspensions: ISPVP-SDBS-SWNTs were diluted at a final concentration of 1 mg/L in 10× phosphate buffered saline (PBS). Neither the suspension stability nor the luminescence was affected by this treatment (Figure 7a). The combination of the previous experimental findings suggests that ISPVP-SDBS-SWNTs suspensions should be highly effective materials in cellular environments.

To this end, we exposed live cultured HEK293 cells to ISPVP-SDBS-SWNTs suspensions, either for 5 min at room temperature or overnight at 37 °C. Figure 7b,c shows the examples of near-IR luminescence images of a cell recorded at two different foci after 5 min of SWNT incubation. The images were acquired in the presence of white light to identify the outline of the cell. Highly luminescent and diffraction limited spots that likely originated from individualized SWNTs interacting with the surface of the cells were found, as expected because of the positive charge carried by PVP. To assess as to whether the luminescent spots originated from individual tubes, we first checked that the spots displayed a polarized absorption as evidenced by using a rotating linearly polarized excitation[35] (not shown). Second, the narrow spectra originating from luminescent spots found at the surface of the cells (Figure 7d) further support the presence of individual SWNTs.[35] Comparable results were obtained after the 12 h incubation procedure at 37 °C, indicating that ISPVP-SDBS-SWNTs remain perfectly suspended in a biological environment. Further studies will be needed to address the question of cytotoxicity of such materials, but we can envision from our results, together with the known biocompatibility of PVP,[41] that ISPVP-SDBS-SWNTs should be advantageous in biological applications.

Conclusion

By studying the spectroscopic and structural behavior of mixtures of anionic surfactant and PVP polymers at various pH values, we have identified a mixture (ISPVP-SDBS) that might serve as a universal wrapping agent of individual SWNTs. Because of its effectiveness at all pH values, in high saline environments as well as in physiological medium, we foresee an extensive use of ISPVP-SDBS-SWNTs in fields as varied as chemistry, physics, and biology for fundamental research as well as more applied technologies.

Experimental Procedures

Preparation of Suspensions. Suspensions of HiPco tubes were dispersed in one weight percent (wt %) anionic (SDBS, $C_{18}H_{29}O_3SNa$; SDS, $C_{12}H_{25}O_4SNa$), neutral (Pluronics (F88, $(C_5H_{10}O_2)_n$)), or cationic (cetyl trimethyl ammonium bromide (CTAB, $C_{19}H_{42}NBr$)) surfactants as well as in polymers (PVP, $(C_6H_8ON)_n$) alone using homogenization, ultrasonication, and ultracentrifugation following standard literature methods.[8] All suspensions were characterized spectroscopically and by atomic force microscopy (AFM) to ensure that the SWNTs were predominantly suspended as individuals. Suspensions in SDBS, SDS, Pluronic, and CTAB were also added to 1 wt % PVP or 1 wt % VP to obtain suspensions of mixed wrapping agents. The surfactant-polymer molar ratio was maintained above the cmc for all surfactants used (SDBS, cmc = 1.6 mM; SDS, cmc = 8.35 mM; F88, cmc = 1.6 mM; and CTAB, cmc = 1.3 mM). Suspensions of mixed wrapping agents were prepared using one part SWNT-surfactant and three parts PVP to result in a final concentration of 10 mg/L SWNT, 0.25 wt % surfactant, and 0.75 wt % PVP or VP. All spectroscopy measurements were performed on 1 mL samples in a sterile cuvette.

Optical Ensemble Measurements. Fluorescence, absorbance, and liquid-phase Raman measurements were first performed on solutions at neutral pH values. Successive additions of 1 μL aliquots of 1 M

(39) Kang, Y. J.; Taton, T. A. *J. Am. Chem. Soc.* **2003**, *125*, 5650−5651.
(40) Wang, R.; Cherukuri, P.; Duque, J. G.; Leeuw, T. K.; Lackey, M. K.; Moran, C. H.; Moore, V. C.; Conyers, J. L.; Smalley, R. E.; Schmidt, H. K.; Weisman, B. R.; Engel, P. S. *Carbon* **2007**, *45*, 2388−2393.
(41) Guowei, D.; Adriane, K.; Chen, X.; Jie, C.; Yinfeng, L. *Int. J. Pharm.* **2007**, *328*, 78−85.

hydrochloric acid (HCl) or 1 M KOH were then added until the desired pH was reached. Bulk fluorescence and absorbance measurements were measured with a Nanospectralyzer Model NS1, version 1.97 (Applied Nanofluorescence). The SWNT fluorescence was excited at 660 nm, and emission was detected between 900 and 1400 nm. Absorbance was measured in the visible and near-IR (400−1400 nm); integration times of 500 ms and 10 accumulations were used in both cases. Absorbance at 763 nm was used to normalize the fluorescence spectra. Liquid-phase Raman spectroscopy was performed using a 785 nm laser excitation in a Renishaw system fitted with a microscope. Spectra were collected with a Renishaw Raman Macro Sampling Set (Wire 2 software) between 100 and 3200 cm^{-1} with a 10 s exposure time and 1 accumulation. Time-dependent luminescence spectra of SWNT suspensions in SDBS, PVP, or PVP-SDBS were taken every 0.5 s (50 ms exposure time and 6 accumulations) using a 660 nm laser excitation. Successive measurements began immediately after a SWNT suspension at neutral pH was injected into 10 μL of 1 M HCl.

Near-IR Fluorescence Microscopy of Individual SWNTs. Individual semiconducting SWNTs were visualized by near-IR fluorescence microscopy. Prior to imaging, a 5 μL drop of nanotube suspension was placed between a glass slide and a microscope coverslip sealed with silicon grease to prevent drying. SWNT samples were mounted onto an inverted epifluorescence microscope (Nikon TE-2000) equipped with a 60× oil emersion objective (NA = 1.4, Nikon). Samples were continuously excited by a circularly polarized beam of a 658 nm diode laser. The infrared photoluminescence emitted by the SWNTs passed through long-pass infrared filters (LP950, Thorlabs) and was detected by a liquid nitrogen-cooled camera (16-bit InGaAs 2D array, OMA-V 2D, Princeton Instruments). Single frame acquisition images of the SWNT luminescence were recorded with an integration time of 50 ms.[35]

Cell Culture and Preparation for Microscopy. HEK293 cells were cultured on microscope cover slips in DMEM medium supplemented with streptomycin (100 μg/mL), penicillin (100 U/mL), and 10% bovine serum in a humidified atmosphere (95%) at 5% CO_2 and 37 °C. Cells were used for 12−14 passages and were transferred every 4−6 days. Cells were exposed to 50 μL of VP-SDBS-SWNTs suspension (of 1 μg/mL added to 1.5 mL of culture medium) for either 5 min at room temperature or 12 h at 37 °C. The cells were then washed with fresh medium. The cover slips were mounted in a custom chamber with culture medium, and all data were taken at room temperature.

AFM. AFM images were taken using a Nanoscope IIIa system (Veeco/Digital Instruments) in tapping mode at a scan rate of 2 Hz and scan size of 10 μm. A total of 20 μL of SWNT suspensions was spin coated at 3000 rpm onto a freshly cleaved mica surface (Ted Pella, Inc.) and rinsed with DI water.

Lyophilization and Resuspension of ISPVP-SDBS-SWNT. Lyophilization was performed using a Freezemobile 3+SL (The Virtis Company). A total of 1 mL of ISPVP-SDBS-SWNT was freeze-dried at −40 °C for 12 h. Resuspension was accomplished by the addition of 1 mL of DI water and mild shaking.

Acknowledgment. The authors thank Amanda L. Higginbotham for helpful discussions, Ramsey I. Kamar and Robert M. Raphael for providing the HEK cells, Dmitry A. Tsyboulski for help with the collection of 2-D contour plots, and R. Bruce Weisman for providing access to his laboratory and near-IR fluorescence imaging facilities. This work was supported by the Robert A. Welch Foundation (C-1668) and the NSF Center for Biological and Environmental Nanotechnology (EEC-0118007 and EEC-0647452). L.C. thanks the Fulbright Foundation and the DGA (ERE060016) for financial support.

Supporting Information Available: Cryo-TEM images of SWNTs at pH 2 and 7. In situ polymerization of VP conducted under acidic conditions. Fluorescence intensity of the ISPVP-SDBS-SWNTs after polymerization. This material is available free of charge via the Internet at http://pubs.acs.org.

JA0777234